Polyhedron Vol. 10, No. 20/21, pp. 2423–2435, 1991
Printed in Great Britain

0277–5387/91 \$3.00+.00

UNEXPECTED REACTION OF $[Ni(CO)_{4-n}(R_2PCl)_n]$ ($n = 1, 2$; $R = Bu^t$, Cy, Ph) WITH $Na_2[Fe_2(CO)_8]$. SYNTHESIS AND ELECTRONIC STRUCTURE OF THE ANIONS $[Fe_2(\mu\text{-}CO)(CO)_6(\mu\text{-}PR_2)]^-$ AND THEIR REACTIONS WITH H^+ AND $[M(PPh_3)]^+$ ($M = Cu, Ag, Au$)

BERNHARD WALTHER,* HELMUT HARTUNG, HANS-C. BÖTTCHER,
UTE BAUMEISTER and UWE BÖHLAND

Department of Chemistry, Martin Luther University, Halle-Wittenberg, Weinbergweg 16,
O-4050 Halle/S., Germany

and

JOACHIM REINHOLD and JOACHIM SIELER

Department of Chemistry, University of Leipzig, Talstr. 35, O-7010 Leipzig, Germany

and

JEAN LADRIERE

Inorganic and Nuclear Chemistry Laboratory, University of Louvain, 2,
Chemin du Cyclotron, B-1348 Louvain-la-Neuve, Belgium

and

HANS-MARTIN SCHIEBEL

Department of Organic Chemistry, Technical University Braunschweig, Hagenring 30,
W-3300 Braunschweig, Germany

(*Received* 23 *April* 1991; *accepted* 2 *July* 1991)

Abstract—Treatment of $[Ni(CO)_{4-n}(R_2PCl)_n]$ ($n = 1, 2$; $R = Bu^t$, Cy, Ph) with $Na_2[Fe_2(CO)_8]$ gave, depending on *n* and R, either the doubly phosphido-bridged complexes $[Fe_2(CO)_6(\mu\text{-}PR_2)_2]$ or the anions $[Fe_2(\mu\text{-}CO)(CO)_6(\mu\text{-}PR_2)]^-$. These anions can also be obtained by the reaction of $[Fe(CO)_4(PR_2)]^-$ with either $[Fe_2(CO)_9]$ or $[Fe(CO)_5]$ via the intermediate $[Fe_2(CO)_8(\mu\text{-}PR_2)]^-$. The electronic structure of the anions $[Fe_2(\mu\text{-}CO)(CO)_6(\mu\text{-}PR_2)]^-$ has been studied by an EHT calculation which supports their ambident oxygen- or metal-nucleophilicity. The metal-centred nucleophilic reactions of the anion $[Fe_2(\mu\text{-}CO)(CO)_6(\mu\text{-}PBu^t_2)]^-$ with H^+ and $[M(PPh_3)]^+$, ($M = Cu, Ag, Au$), respectively, are described. The new complexes have been characterized by various spectroscopic methods and the structure of $[Fe_2\{\mu\text{-}Ag(PPh_3)\}(\mu\text{-}CO)(CO)_6(\mu\text{-}PBu^t_2)]$ has been established by X-ray analysis.

Phosphido-bridged di-iron anions of type $[Fe_2(\mu\text{-}CO)(CO)_6(\mu\text{-}PR_2)]^-$ first reported by Osterloh[1] in 1982 ($R = Ph$), obviously offer a wealth of reactivity. Baker *et al.*[2–4] have recently reported oxidation with $[Fecp_2][BF_4]$ to give a new family of 33e dinuclear radicals $[Fe_2(CO)_7(\mu\text{-}PR_2)]$, which has been extensively investigated by electron spin resonance and molecular orbital studies, ligand substitution reactions as well as structural and electrochemical studies. The same authors described

---

* Author to whom correspondence should be addressed.

substitution reactions which lead by opening the iron–iron bond to disubstituted di-iron complexes $NEt_4[Fe_2(CO)_6L_2(\mu\text{-}PPh_2)]$ (L = PPh_3, PMe_3, $P(OMe)_3$). Photolysis of these complexes results in ligand loss and formation of the substituted anionic complexes $NEt_4[Fe_2(\mu\text{-}CO)(CO)_5L(\mu\text{-}PPh_2)]$ and $NEt_4[Fe_2(\mu\text{-}CO)(CO)_4L_2(\mu\text{-}PPh_2)]$, respectively. We expect these anions to have ambident nucleophilic reactivity as described in structures A and B.

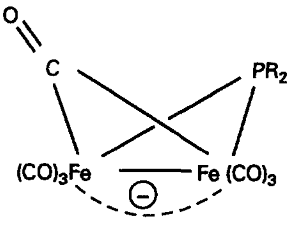

A

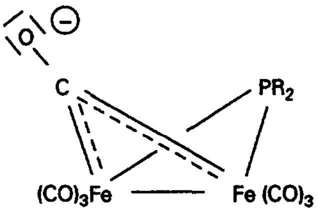

B

Osterloh[1] found that the oxygen-based nucleophilic reaction with $[R_3O][BF_4]$ afforded alkoxymethylidine complexes $[Fe_2(CO)_6(\mu\text{-}COR)(\mu\text{-}PPh_2)]$ which isomerized on heating into the acyl complexes $[Fe_2(CO)_6(\mu\text{-}\eta^2\text{-}COR)(\mu\text{-}PPh_2)]$.

In this paper we show that the reaction of chlorophosphane-substituted nickel carbonyl complexes with the di-iron octacarbonyl dianion does not give heteronuclear iron–nickel complexes but gives either $[Fe_2(CO)_6(\mu\text{-}PR_2)_2]$ or $Na[Fe_2(\mu\text{-}CO)(CO)_6(\mu\text{-}PR_2)]$. A new synthesis of the di-iron anions $[Fe_2(CO)_7(\mu\text{-}PR_2)]^-$ is presented. The metal-based nucleophilic reactions of the anionic complex $Na[Fe_2(\mu\text{-}CO)(CO)_6(\mu\text{-}PBu^t_2)]$ with the electrophilic agents H^+ and $[M(PPh_3)]^+$ (M = Cu, Ag, Au) to yield the hydride complex and the triangular Fe_2M clusters of the coinage metals, respectively, are described. The structure of the Fe_2Ag cluster has been determined by X-ray crystal analysis. In order to come to a better understanding of the bonding properties of the di-iron anions an EHMO calculation on the model anion $[Fe_2(\mu\text{-}CO)(CO)_6(\mu\text{-}PH_2)]^-$ has been performed.

EXPERIMENTAL

All reactions were performed under oxygen-free argon using conventional Schlenk techniques. Solvents were dried over molecular sieves or over sodium/benzophenone ketyl and distilled under argon prior to use. Melting points were recorded in sealed capillaries under argon and are uncorrected. Starting materials were either commercially available or were prepared according to literature procedures: Bu^t_2PCl,[5] Cy_2PCl,[6] Ph_2PCl,[7] Me_2PCl,[8] $Na_2[Fe_2(CO)_8]$,[9] $Na_2[Fe(CO)_4]\cdot 1.5C_4H_8O_2$,[10] [PPN]Cl,[11] $[\{CuCl(PPh_3)\}_4]$,[12] $[\{AgCl(PPh_3)\}_4]$,[13] $[AuCl(PPh_3)]$.[14]

IR spectra were obtained using an IR 71 of VEB Carl Zeiss Jena. ^1H and ^{31}P NMR spectra were recorded on the Bruker spectrometers WP 200 (^1H at 200.1 MHz, ^{31}P at 81.0 MHz) and AC 80 (^1H at 80.1 MHz, ^{31}P at 32.4 MHz). Chemical shift references are the absolute frequencies of Me_4Si (^1H) and external 85% $H_3PO_4(aq)$(^{31}P), respectively. Positive shifts are to lower field. The EI mass spectra were obtained with a Hewlett Packard spectrometer 5995 A. FAB MS were obtained with a Finnigan MAT 8430 instrument (Bremen, Germany). Xenon was used for neutral beam production with a beam energy of 8 kV. 3-Nitrobenzylalkohol (NBA) and 2-nitro-*n*-octylether (NOE), respectively, were used as liquid matrix. Mössbauer spectra were recorded at room temperature using a constant acceleration spectrometer with a source of ^{57}Co in rhodium. All isomer shifts are quoted relative to natural iron at room temperature. Absorbers containing less than 10 mg cm^{-2} of natural iron were used for all spectra. The spectra have been fitted to Lorentzian line shapes using an iterative least-squares program. The intensity of the quadrupole doublets were constrained to be equal which is a good assumption for a powdered random sample. The relative proportions of the different components were calculated from peak areas, assuming that all iron species have similar Lamb–Mössbauer factors, which could give rise to an inaccuracy of ±5%.

$[Ni(CO)_{4-n}(R_2PCl)_n]$ (**1a–c**, **2a**,**b**)

These complexes were synthesized according to the procedure used by Ehrl and Vahrencamp[15] for the synthesis of $[Ni(CO)_3(Me_2PCl)]$ by stirring *ca* 10 mmol $[Ni(CO)_4]$ with R_2PCl in the appropriate molar ratio (**1** : 1 : 2 ; **2** : 1 : 1) in diethylether, usually at room temperature in the dark for 1 h (**2**) and 3 h (**1**), respectively. Only the synthesis of **1a** requires refluxing for an additional 4 h after having stirred the mixture for 1 h at room temperature. The CO evolution was monitored by gas volumetric measurements. Subsequently, all volatile materials were removed *in vacuo*, and the residue was dissolved in a minimum quantity of pentane (*ca* 5–10 cm^3). The cold solvent was decanted off, and the white crystals were dried *in vacuo*, keeping them cold and in the dark. The yield is about 80%. Complexes **1** and **2** proved to be fairly unstable both thermally and photolytically and have to be stored below 0°C. $[Ni(CO)_3(Ph_2PCl)]$ appeared too unstable for separation. The analytical and physical data are summarized in Table 1.

Reaction of $[Ni(CO)_2(Bu^t_2PCl)_2]$ (**1a**) *with* $Na_2[Fe_2(CO)_8]$

Complex **1a** (0.48 g, 1 mmol) was added to a suspension of $Na_2[Fe_2(CO)_2]$ (0.38 g, 1 mmol) in 20 cm^3 THF and stirred in the dark at room temperature for 5 h. The deep red–brown mixture was filtered and the solvent was removed *in vacuo*. The sticky residue became microcrystalline by stirring in pentane. After repeated extractions with small amounts of pentane until the solvent remained colourless, the crystals were collected by filtration and dried *in vacuo*. Yield 0.48 g Na[**3a**] (~ 100%). Characterization s. below. The other reactions, summarized in eq. (1), were carried out similarly.

Preparation of Na(K,PPN)[**3a–d**]

(A) An equimolar amount of R_2PCl (0.36 g Bu_2^tPCl, 0.46 g Cy_2PCl, 0.43 g Ph_2PCl, 0.19 g Me_2PCl) was added dropwise to a suspension of 0.69 g (2 mmol) $Na_2[Fe(CO)_4]\cdot 1.5$ dioxane in 30 cm^3 THF, and the mixture was stirred for 2 h. The bright yellow solution changed colour to red–brown after the addition of $[Fe(CO)_5]$ (0.27 cm^3, 2 mmol) or $[Fe_2(CO)_9]$ (0.72 g, 2 mmol), respectively. On stirring for 24 h, the solution was irradiated (Hg lamp) for 5 h. During this time the colour turned deep brown. The reaction mixture was subsequently evaporated to dryness under reduced pressure and the residue suspended in 20 cm^3 pentane, filtered and then washed with an additional 20 cm^3 pentane. After drying *in vacuo* the microcrystalline pyrophoric solids Na(K)[**3a–d**] (yield nearly 100%) were used directly for further reactions, or were dissolved in 10 cm^3 degassed methanol, filtered and the filtrate treated with 1.15 g (2.1 mmol) [PPN]Cl. The resulting crystals of PPN[**3a–d**] were collected by filtration, washed with methanol and dried *in vacuo*.

(B) A solution of 0.72 g (2 mmol) $[Fe_2(CO)_9]$ and an equimolar amount of R_2PH (0.37 g Bu_2^tPH, 0.37 g Ph_2PH) in 30 cm^3 THF were stirred at room temperature for 2 h. The solvent and the $[Fe(CO)_5]$ formed during reaction were removed *in vacuo*, and the residue was redissolved in 30 cm^3 THF. This solution was treated with an excess of KH (*ca* 0.1 g) for 2 h, giving a deep red solution of $K[Fe(CO)_4(PR_2)]$ which was filtered and handled after addition of 0.72 g (2 mmol) $[Fe_2(CO)_9]$ as described above. The yields were similar to method A. Complexes Na(K)[**3a–d**] were highly air sensitive in both solid state and solution whereas PPN[**3a–d**] are stable as solids but moderately air sensitive in solution.

Table 1. Analytical and physical data of $[Ni(CO)_{4-n}(R_2PCl)_n]$ ($n = 2$, **1a–c**; $n = 1$, **2a,b**)

Compound	M.p. (dec.) (°C)	Analytical data[a] C	H	Cl	P	NMR data (ppm)[b] ^1H	^{31}P	IR $\nu(CO)$ (cm^{-1})
1a $[Ni(CO)_2(Bu_2^tPCl)_2]$	97–101	45.2 (45.4)	7.0 (6.8)	14.6 (14.9)	13.1 (13.0)	1.33d[c]	177.26s	2000(s), 1942(s)[e]
1b $[Ni(CO)_2(Cy_2PCl)_2]$	101–104	53.4 (53.8)	7.9 (7.6)	12.2 (12.2)	10.4 (10.6)		154.5s	2011(s), 1950(s)[e]
1c $[Ni(CO)_2(Ph_2PCl)_2]$	99–101	55.7 (56.1)	4.0 (3.6)	12.5 (12.8)	11.1 (11.1)		110.0s	2004(s), 1946(s)[e]
2a $[Ni(CO)_3(Bu_2^tPCl)]$	~ 10	41.0 (40.8)	5.4 (5.6)	11.2 (11.0)	9.3 (9.6)	1.05d[d]	175.95s	2065(s), 1990(s), 1985(s)[f]
2b $[Ni(CO)_3(Cy_2PCl)]$	48–50	47.9 (48.0)	6.3 (5.9)	10.0 (9.4)	8.2 (8.2)		150.0s	2075(s), 1990(s), 1955(d)[f]

[a] Calculated figures in parentheses.
[b] ^1H: C_6D_6; ^{31}P: C_6D_6.
[c] $^3J(PH)$ 13.6 Hz.
[d] $^3J(PH)$ 14.9 Hz.
[e] Nujol mull.
[f] Pentane.

Table 2. Analytical and physical data of PPN[**3a–d**]

Compound		Colour	Yield, g (%)	M.p. (dec.) (°C)	Analytical data[a] C	H	N	P
PPN[**3a**]	PPN[Fe$_2$(CO)$_7$(μ-PBu$_2^t$)]	brick-red	1.60 (80)	138–140	61.6 (61.8)	4.9 (4.9)	1.4 (1.4)	9.6 (9.4)
PPN[**3b**]	PPN[Fe$_2$(CO)$_7$(μ-PCy$_2$)]	brown	1.25 (60)	134–136	63.8 (63.3)	4.7 (5.0)	1.4 (1.3)	9.3 (8.9)
PPN[**3c**]	PPN[Fe$_2$(CO)$_7$(μ-PPh$_2$)]	deep red	1.64 (80)	121–123	63.1 (64.6)	4.1 (3.9)	1.5 (1.3)	8.9 (9.0)
PPN[**3d**]	PPN[Fe$_2$(CO)$_7$(μ-PMe$_2$)]	orange–yellow	1.10 (60)	130–135	59.1 (59.5)	4.2 (4.0)	1.6 (1.5)	10.4 (10.0)
4a	[Fe$_2$(CO)$_7$(H)(μ-PBu$_2^t$)]	deep red	0.34 (75)	89	40.0 (39.7)	4.5 (4.2)		6.4 (6.8)
5	[Fe$_2$(μ-CuPPh$_3$)(CO)$_7$(μ-PBu$_2^t$)]	red–violet	0.20 (25)	146–148	50.6 (50.9)	4.3 (4.3)		7.6 (7.9)
6	[Fe$_2$(μ-AgPPh$_3$)(CO)$_7$(μ-PBu$_2^t$)]	red–violet	0.42 (51)	172–175	48.3 (48.1)	4.1 (4.0)		7.2 (7.5)
7	[Fe$_2$(μ-AuPPh$_3$)(CO)$_7$(μ-PBu$_2^t$)]	red–violet	0.57 (62)	179–182	43.0 (43.4)	3.7 (3.6)		6.4 (6.8)

[a] Calculated figures in parentheses.

These complexes are well soluble in THF and CH$_2$Cl$_2$ but not in diethylether and hexane. Analytical and physical data of PPN[**3a–d**] are given in Table 2.

[Fe$_2$(CO)$_7$(H)(μ-PBu$_2^t$)] (**4a**)

A solution of Na[Fe$_2$(CO)$_7$(μ-PBu$_2^t$)] (**3a**) (0.48 g, 1 mmol) and CH$_3$COOH (0.12 g, 2 mmol) in *ca* 20 cm^3 THF was rigorously stirred for 30 min. Subsequently, the solvent was removed *in vacuo*, and the residue was three times extracted with 10 cm^3 pentane. The combined extracts were filtered and evaporated *in vacuo* until 5 cm^3 remained. Deep red crystals of **4a** were obtained at -78°C. Further details are given in Table 2.

[Fe$_2$(CO)$_7$(H)(μ-PPh$_2$)] (**4c**)

The solution of NEt$_4$[**3c**] (0.62 g, 1 mmol) and CF$_3$COOH (0.23 g, 2 mmol) in 30 cm^3 THF was stirred for 3 h. The solvent was removed *in vacuo* and the residue was extracted three times with 10 cm^3 pentane. Evaporation of the filtered pentane extracts gave a deep red oily material (m.p. <-40°C) which was characterized by spectroscopic means.

Air-oxidation of complex **4c**

Dried air was bubbled through a THF solution of **4c** for 1 h. The solution was filtered, and the solvent was removed *in vacuo*. The residue was three times extracted with pentane, and the combined extracts were reduced *in vacuo* to 5 cm^3. [Fe$_2$(CO)$_6$(μ-OH)(μ-PPh$_2$)] crystallized at -78°C. M.p. 123°C (dec.). IR (hexane, cm^{-1}): 2073 (vs), 2070 (m, sh), 2033 (vs), 2000 (s), 1994 (s), 1984 (s, sh), 1977 (vs). ^{1}H NMR (CD$_2$Cl$_2$): δ -2.16 (d, ^3J(PH) 11.8 Hz, FeH), 7.5 (m, Ph). ^{31}P NMR (CHCl$_3$): δ 121.8 s.

[Fe$_2${μ-M(PPh$_3$)}(μ-CO)(CO)$_6$(μ-PBu$_2^t$)] (M = Cu, **5**; Ag, **6**; Au, **7**)

The suspension of Na[**3a**] (0.72 g, 1.5 mmol) and [MCl(PPh$_3$)] (0.36 g (Cu), 0.41 g (Ag), 0.5 g (Au), 1 mmol) in 30 cm^3 THF was stirred at room temperature in the dark for 5 (Cu), 4 (Ag), and 3 (Au) h, respectively. After filtration, the solution was evaporated to dryness, the residue washed with pentane, and repeatedly extracted with small amounts of diethylether until the ether remains nearly colourless. Complexes **5–7** crystallize from these solutions at -30°C. **5** and **6** require purification by repeated recrystallization from pentane/diethylether mixture. For further details and analytical data see Table 2.

X-ray analysis of **6**

Crystal data. C$_{33}$H$_{33}$AgFe$_2$O$_7$P$_2$, F.W. = 823.1, triclinic, space group $P\bar{1}$, $a = 12.714(2)$, $b = 14.667(2)$, $c = 10.121(2)$ Å, $\alpha = 96.79(1)$, $\beta =$

113.14(1), $\gamma = 88.68(1)°$, $V = 1722.6(4)$ Å^3, $Z = 2$, $D_{calc} = 1.59$ g cm^{-3}, $F(000) = 832$, λ(Mo-K_α) = 0.71069 Å, μ(Mo-K_α) = 15.2 cm^{-1}.

Measurements. A red cubic crystal with approximate dimensions $0.15 \times 0.15 \times 0.15$ mm was mounted in a glass capillary. All measurements were done on a Rigaku AFC6R diffractometer with graphite monochromated Mo-K_α radiation at 296 K. Cell constants and orientation matrix were obtained from a least-squares treatment of the setting angles for 25 reflections in the range $37.8 < 2\theta < 43.2°$. Intensity data were measured using the ω–2θ scan technique up to 50° in 2θ. A total of 6334 reflections delivered a set of 6036 unique intensity data ($R_{int} = 0.039$), 4026 of them were considered observed ($I \geqslant 3.00\sigma(I)$). Lorentz and polarization corrections were applied during the process of data reduction.

Solution and refinement of the structure. The structure was solved by direct methods[16,17] and refined by full-matrix least-squares techniques with anisotropic displacement parameters for the non-H atoms. The displacement parameters of the H-atoms all found in a difference map were refined isotropically. For the refinement 9.17 reflections/parameter were available. The applied weighting scheme was based on counting statistics and included a factor to downweight the intense reflections. The final R was 0.048 ($R_w = 0.056$). A final difference map had maximum peak heights of 1.11 and -1.31 e Å^{-3}, respectively. The maximum shift/error ratio in the last l.s. cycle was 0.01. Scattering factors including corrections for anomalous dispersion effects were taken from ref. 18. All calculations were performed using the TEXSAN[19] crystallographic software package of Molecular Structure Corporation. Tables of atomic coordinates and displacement parameters, lists of observed and calculated structure factors as well as a complete list of bond lengths and angles have been deposited with the editor, atomic coordinates also with the Cambridge Crystallographic Data Centre.

RESULTS AND DISCUSSION

Synthesis

In an attempt to prepare the electron precise heteronuclear cluster $[Fe_2Ni(CO)_8(\mu\text{-}PBu^t_2)_2]$ by "bridge-assisted" synthesis from $[Ni(CO)_2(Bu^t_2PCl)_2]$ (**1a**) and $Na_2[Fe_2(CO)_8]$ in tetrahydrofurane we unexpectedly obtained the di-iron anion $[Fe_2(\mu\text{-}CO)(CO)_6(\mu\text{-}PBu^t_2)]^-$ (**3a**) as the sodium salt Na[**3a**]. This result prompted further investigation of the reaction of $[Ni(CO)_{4-n}(R_2PCl)_n]$ ($n = 2$, **1**; $n = 1$, **2**) with $Na_2[Fe_2(CO)_8]$. Thus, complexes **1b**,**c** gave under analogous conditions the well-known neutral bis(phosphido)-bridged di-iron complexes $[Fe_2(CO)_6(\mu\text{-}PR_2)_2]$. On the other hand, treatment of the monosubstituted nickel carbonyl complexes **2** with $Na_2[Fe_2(CO)_8]$ showed no reaction with **2a** and the formation of Na[**3b**] from **2b**, respectively. The reactions discussed are summarized in eq. (1).

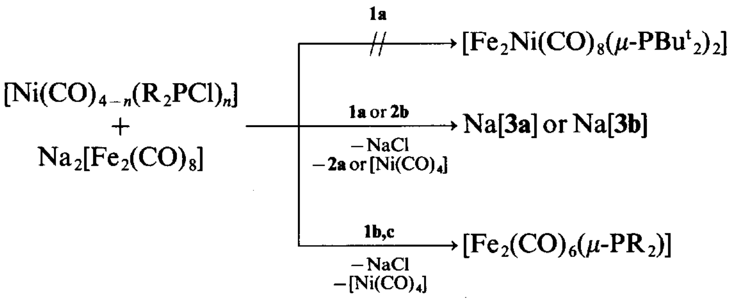

(1)

R	Bu^t	Cy	Ph	Me
	a	b	c	d

(throughout this work)

These reactions show (i) distinct differences in the reactivity of $[Ni(CO)_{4-n}(R_2PCl)_n]$ with $Na_2[Fe_2(CO)_8]$ depending on n and R and (ii) that they neither provide heteronuclear FeNi complexes nor a general procedure for the phosphido-bridged di-iron anions **3**.

The mechanism of these reactions remains unknown. However, in summary, one or two ligand exchange steps of R_2PCl for CO occur to give $[Ni(CO)_{5-n}(R_2PCl)_{n-1}]$ and Na[**3**] or $[Fe_2(CO)_6(\mu\text{-}PR_2)_2]$. The latter two products are formed by conversion of R_2PCl into the R_2P^- ligand through

NaCl elimination. The $[Ni(CO)_{5-n}(R_2PCl)_{n-1}]$ by-products were either detected *in situ* by ^{31}P NMR ($n = 2$) or by IR spectroscopy ($n = 1$) as constituents of the volatile material obtained by evacuation of the reaction mixture. $NEt_4[Fe_2(\mu\text{-}CO)(CO)_6(\mu\text{-}PPh_2)]$, obviously an anionic complex of type **3**, had already been synthesized by Osterloh[1] in 1982 by treatment of $(NEt_4)_2[Fe_2(CO)_8]$ with Ph_2PCl via $NEt_4[Fe_2(CO)_8(\mu\text{-}PPh_2)]$ as an isolable intermediate. This procedure has later been used by Baker *et al.*[3] for the *in situ* preparation of the di-iron anions **3** with R = Et, Ph, Cy, Bu^t. To our knowledge, the preparation and characterization of these anionic di-iron complexes have not yet been published. This, together with the poor yields of anions **3** [isolated as bis(triphenylphosphane)immonium (PPN^+) salts] we obtained by reacting R_2PCl with $Na_2[Fe_2(CO)_8]$ (PPN[**3a**] 45%, PPN[**3b**] zero %, PPN[**3c**] 10%), lead us to suggest a synthetic method on the basis of the anion $[Fe(CO)_4(PR_2)]^-$ as outlined in eq. (2).

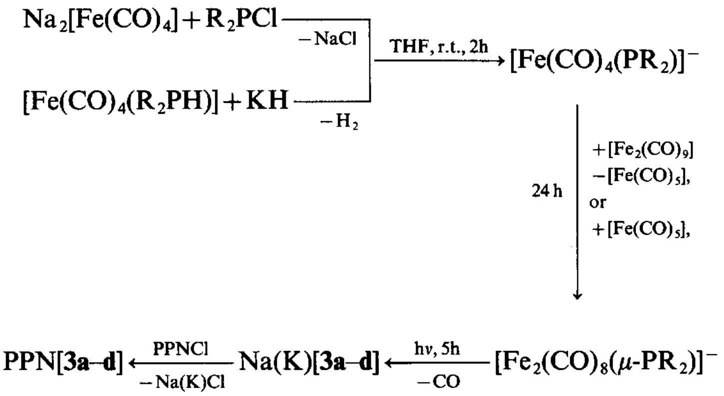

(2)

The protonation reaction of anionic binuclear complexes and clusters has been frequently employed to produce neutral hydride complexes. Accordingly, complex Na[**3a**] reacts at room temperature in THF with acetic acid to afford crystalline $[Fe_2(\mu\text{-}CO)(CO)_6(H)(\mu\text{-}PBu^t_2)]$ (**4a**) in good yield.

Although the spectroscopic data of complex **4a** (see below) do not allow a decision concerning the coordination mode of the hydride ligand (terminal or bridging) the observed high-field shift for this ligand in the ^1H NMR spectrum gives evidence for a direct iron–hydrogen bond. This result is of interest in the light of the reports on related complexes in the literature. In 1972 Treichel *et al.*[20] reported the synthesis of complexes $[Fe_2(CO)_6(\mu\text{-}H)(\mu\text{-}PR_2)]$ (R = Me, Et, Ph) and one year later found by X-ray analysis of the complex $[Fe_2(CO)_6(\mu\text{-}OH)\{\mu\text{-}P(p\text{-}C_6H_4Me)_2\}]$ that these compounds actually bear a bridging hydroxy ligand.[21] The origin of the oxygen atom remained unknown. Osterloh[1] described, that the reaction of NEt_4[**3c**] with $HBF_4\cdot OEt_2$ in THF gave the same complex $[Fe_2(CO)_6(\mu\text{-}OH)(\mu\text{-}PPh_2)]$ as reported,[20,21] and noted that the mechanism by which this complex is formed is not known.

These results stimulated further investigation of these complexes. Contrary to the $\mu\text{-}PBu^t_2$-bridged anion **3a** the $\mu\text{-}PPh_2$-bridged complexes $Na(NEt_4)$[**3c**] do not react with acetic acid but react readily with CF_3COOH to result under anaerobic conditions a deep red oily material. All attempts to crystallize this compound have failed until now. On the basis of the spectroscopic data, this complex is assigned an analogous constitution $[Fe_2(\mu\text{-}CO)(CO)_6(H)(\mu\text{-}PPh_2)]$ (**4c**) to that of the hydride complex **4a**.

Evidence that the above-mentioned μ-OH bridged complexes were formed by air-oxidation of the hydride complexes in the course of their preparation[1,20] comes from the systematic oxidation of the hydride **4c**. Bubbling dry air through a THF solution of this hydride for 1 h gave orange–red $[Fe_2(CO)_6(\mu\text{-}OH)(\mu\text{-}PPh_2)]$ which was identified by identical IR, ^1H and ^{31}P NMR data with those previously reported.[1,20]

Treatment of the THF solution of Na[**3a**] with the electrophilic complexes $[\{MCl(PPh_3)\}_n]$ (M = Cu, Ag, $n = 4$; M = Au, $n = 1$) yielded the triangular 46e clusters $[Fe_2\{\mu\text{-}M(PPh_3)\}(\mu\text{-}CO)(CO)_6(\mu\text{-}PBu^t_2)]$ (M = Cu, **5**; Ag, **6**; Au, **7**) as deep red–violet crystals. Similar coinage metal clusters have very recently been reported by another group.[22]

Spectroscopy

The new complexes were characterized by elemental analysis (see Experimental) as well as by IR, ^1H, $^{31}P\{^1H\}$ NMR (Table 3), and mass spec-

Table 3. Spectroscopic data of complexes PPN[**3a–d**] and **4a,c**

Complex	IR (cm^{-1})^a		^{1}H NMR		^{31}P NMR	
	ν(t-CO)	$\nu(\mu$-CO)	δ (ppm)	$^{2/3}J$(PH), Hz	δ (ppm)	^3J(PP), Hz
PPN[**3a**] PPN$[\mathrm{Fe_2(CO)_7}(\mu\text{-PBu}^t_2)]$	2000(vs), 1952(vs,br), 1902(s,br), 1880(w)	1720(vs)	1.43d(PBu$^t_2$)^b 7.6br(PPN)	13.0	239.5s^b	
PPN[**3b**] PPN$[\mathrm{Fe_2(CO)_7}(\mu\text{-PCy}_2)]$	2004(vs), 1950(vs), 1914(s), 1888(s)	1724(vs)			160.2s^b	
PPN[**3c**] PPN$[\mathrm{Fe_2(CO)_7}(\mu\text{-PPh}_2)]$	2016(vs), 1964(vs,br), 1928(s), 1904(w), 1892(w)	1724(vs)			125.3s^b	
PPN[**3d**] PPN$[\mathrm{Fe_2(CO)_7}(\mu\text{-PMe}_2)]$	2008(vs), 1956(s), 1920(s), 1904(vs), 1880(vw)	1716(vs)	1.85d(PMe$_2$)^c 6.9br(PPN)	8.6	100.0^b	
4a $[\mathrm{Fe_2(CO)_7(H)}(\mu\text{-PBu}^t_2)]$	2074(vs), 2040(vs), 2004(s), 1996(s), 1984(vs)	1804(vs)	1.14d(PBu$^t_2$)^d −10.7d(HFe)	13.0 51.0	206.0s^e	
4c $[\mathrm{Fe_2(CO)_7(H)}(\mu\text{-PPh}_2)]$			−10.0d(HFe)^d	54.1	166.0^e	
5 $[\mathrm{Fe_2}(\mu\text{-CuPPh}_3)\mathrm{(CO)_7}(\mu\text{-PBu}^t_2)]$	2032(vs), 1988(s), 1972(s), 1952(w), 1934(s), 1922(s)	1756(vs)	1.35d(PBu$^t_2$)^d	13.8	239.5d(PBu$^t_2$)^e 0.2br(PPh$_3$)	10.4
6 $[\mathrm{Fe_2}(\mu\text{-AgPPh}_3)\mathrm{(CO)_7}(\mu\text{-PBu}^t_2)]$	2028(vs), 1986(m), 1966(s), 1948(w), 1932(s)	1744(vs)	1.4d(PBu$^t_2$)^d	13.8	251.3(PBu$^t_2$)^{e,g} 10.63dd(PPh$_3$)^h 10.23dd(PPh$_3$)^h	9.25
7 $[\mathrm{Fe_2}(\mu\text{-AuPPh}_3)\mathrm{(CO)_7}(\mu\text{-PBu}^t_2)]$	2036(vs), 2000(s), 1968(m), 1956(w), 1940(s,br)	1766(vs)	1.36d(PBu$^t_2$)^d	13.5	243.5d(PBu$^t_2$)^e 52.8d(PPh$_3$)	20.3

[a] Nujol mull.

[b] $\mathrm{CDCl_2}$.

[c] $\mathrm{CH_2Cl_2}$.

[d] $\mathrm{C_6D_6}$.

[e] $\mathrm{C_6H_6}$.

[f] $\mathrm{CD_2Cl_2}$.

[g] Pseudo-triplet, ^2J(AgP) 12.4 Hz (av.).

[h] $J(^{109}\mathrm{AgP})$ 482.8 Hz, $J(^{107}\mathrm{AgP})$ 418.0 Hz.

troscopy. The structure of $[Fe_2\{\mu\text{-}Ag(PPh_3)\}(\mu\text{-}CO)(CO)_6(\mu\text{-}PBu^t_2)]$ (**6**) was determined by X-ray structure determination.

The FAB mass spectra of the anionic complexes PPN[**3a–d**] show in the spectra of the positive ions the $(PPN)^+$ with high abundance (100%). The spectra are nearly matrix-free and display only a few fragments of low abundance (< 10%). In the negative ion mode the characteristic feature of FAB–MS is obtained, i.e. superposition of matrix and sample spectra. The signals of the anions **3a–d** were recorded with a relative abundance in the range of 20–60%. Successive loss of up to three carbonyl ligands is the only degradation process that can be observed. In all cases, for this fragmentation the same course of intensity is displayed, the $(3\text{-}CO)^-$ ion being the most abundant peak. In order to produce this ion it is likely that the bridging carbonyl ligand is being lost to generate a fragment having a formal iron–iron double bond. Ions of the type $(M+3)^-$ and $(M+PPN)^+$, respectively, could not be detected.

Among the $\nu(CO)$ bands of complexes PPN [**3a–c**] that near 1720 cm^{-1} indicates a μ-CO ligand. Similar anions with other bridging ligands have been reported recently, and all of them show a band in the $\nu(\mu\text{-}CO)$ region.[23] The ^{31}P NMR spectra reveal two signals; one at δ 21.0 for the PPN cations, and the other one at low field indicative of phosphido groups bridging a metal–metal bond.[24–26]

The EI mass spectrum of the hydride complex **4a** shows the molecular peak at $m/z = 454$ followed by a sequence of seven peaks arising from the successive loss of all carbonyl ligands. The remaining fragment ion $HFe_2(PBu^t_2)^+$ ($m/z = 258$) appears with relatively high intensity (8.65%), and fragments further by either loss of Bu^t ($m/z = 57$, base peak) or isobutene $C_4H_8^+$ ($m/z = 56 \triangleq Fe^+$) to leave the fragment ions $HFe_2(PBu^t)^+$ ($m/z = 201$) and $H_2Fe_2(PBu^t)^+$ ($m/z = 202$), respectively. The ^{31}P NMR spectrum displays a singlet at low field again indicating that the phosphido ligand bridges the iron–iron bond. The ^1H NMR spectrum consists of two doublets, one for the protons of the μ-PBu^t_2 ligand and the other one at high field for the hydride ligand. The similarity of the structures of **4a** and **4c** is particularly supported by the signals of the hydride ligands at δ *ca* -10 ppm in the ^1H NMR spectra. For the complex $[Fe_2(CO)_6(\mu\text{-}OH)(\mu\text{-}PPh_2)_2]$ proton signals at δ -2.40 ppm (J(PH) 11.5 Hz)[1] and -2.58 ppm (J(PH) 11.0 Hz),[20] respectively, had been assigned to the μ-OH ligand.

The position of the hydride ligand in complexes **4a,c** could not be elucidated with certainty. Therefore it seemed meaningful to investigate the related coinage metal complexes due to the observation that in almost all clusters where structural comparisons are available the $Au(PPh_3)$ unit occupies a similar position to that of the isolobal hydrido ligand in the related hydrido compound.[27]

The coinage metal clusters **5–7** exhibit a similar band pattern in the $\nu(CO)$ region of the IR spectra as do both the starting di-iron anion **3a** and the hydride complex **4a**. Thus five bands appear for terminal CO groups and one for a bridging CO ligand. Due to the positive $M(PPh_3)$ moiety, these bands are shifted to higher wave numbers by about 30 cm^{-1} compared with those of the anionic complex PPN[**3a**]. This could be interpreted in terms of a decrease in the electron density on the iron atoms.

The $^{31}P\{^1H\}$ NMR spectra are as expected, showing one μ-PBu^t_2 environment at low field and one PPh_3 environment. The phosphorus resonance of the PPh_3 ligand coordinated to the M atom appears as a doublet ^3J(PP) for complex **7**, and is split into two double doublets for complex **6** due to both the coupling with ^{109}Ag and ^{107}Ag as well as the ^3J(PP) coupling; for complex **5** this resonance is broad because of the quadrupole moment of the copper nucleus.[28] Accordingly, the signal of the μ-PBu^t_2 ligand appears as a doublet for complexes **5** and **7** ^3J(PP); for complex **6** this resonance appears as a pseudo-triplet due to the superposition of the two double doublets expected from the couplings ^3J(PP) and ^2J(AgP).

The molecular ion of the Fe_2Cu cluster **5** can only be observed in the FAB spectrum of the positive ions. The spectrum is dominated by the matrix and the radical cation $(M)^{+\bullet}$. **5** is detected with less than 5% at m/z 788. Compared with the spectra of complexes **3a–d**, the course of fragmentation is somewhat different. In this case the $(M\text{-}CO)^{+\bullet}$ and the $(M\text{-}3CO)^{+\bullet}$ ions are of very low intensity whereas $(M\text{-}4CO)^{+\bullet}$ provide the base peak in the upper range of the spectrum.

The ^{57}Fe Mössbauer data of compounds PPN[**3a**] and **5–7** are collected in Table 4. The spectra consist of one quadrupole-split doublet corresponding to two equal iron sites which is fully consistent with the crystal structure of the Fe_2Ag cluster **6**. PPN[**3a**] may be thought of as derived from $[Fe_2(CO)_9]$ by replacing two bridging carbonyls by one bridging $Bu^t_2P^-$ ligand. The quadrupole splitting of the anionic complex PPN[**3a**] is roughly three times that observed for $[Fe_2(CO)_9]$ (0.42)[29] but still of the magnitude for a compound with a distorted octahedral environment.[30] A more appropriate description of the coordination sphere around the iron atoms is, ignoring the metal–metal bond, the distorted square pyramid as shown by the X-

Table 4. Room temperature Mössbauer data of complexes PPN[**3a**], **5**–**7**

Complex		δ (mm s^{-1})	ΔE_q (mm s^{-1})	Γ (mm s^{-1})	I (%)
PPN[**3a**]	PPN$[Fe_2(CO)_7(\mu\text{-}PBu^t_2)]$	−0.117	1.290	0.271	65.4[a]
5	$[Fe_2(\mu\text{-}CuPPh_3)(CO)_7(\mu\text{-}PBu^t_2)]$	−0.078	0.986	0.261	100
6	$[Fe_2(\mu\text{-}AgPPh_3)(CO)_7(\mu\text{-}PBu^t_2)]$	−0.050	0.967	0.250	82.07[b]
7	$[Fe_2(\mu\text{-}AuPPh_3)(CO)_7(\mu\text{-}PBu^t_2)]$	−0.050	1.006	0.245	100

[a] Impurity: δ −0.334, ΔE_q 0.847, Γ 0.616, I 34.6.

[b] Impurity: δ +0.10, ΔE_q 0.492, Γ 0.27, I 17.93.

ray crystal structure analysis of $NEt_4[Fe_2(\mu\text{-}CO)(CO)_6(\mu\text{-}PPh_2)]$.[1] The lower isomeric shift of the anion compared with $[Fe_2(CO)_9]$ (0.16)[29] reflects a higher s-electron density on the iron atoms. This is most likely to be caused by an increased s-electron density through phosphorus-to-iron σ-donation although a decrease in the shielding of the s-electrons by decreasing the $3d$ electron density through increased π-back donations should also be taken into account. On going from the anionic complex PPN[**3a**] to the coinage metal complexes **5**–**7** an increase of the isomeric shift is observed. This reflects a decrease in the s-electron density which is qualitatively in accord with the 3c–2e bond description of the $Fe_2(\mu\text{-}Ag)$ core as discussed below.

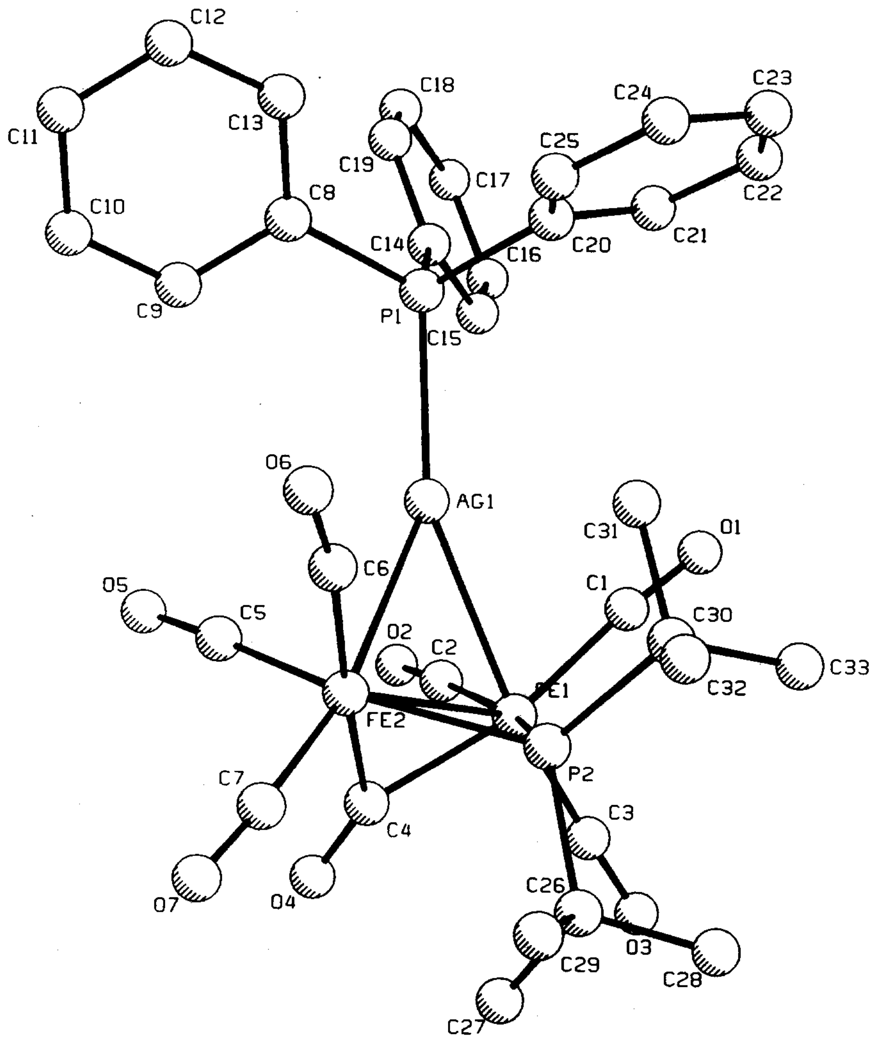

Fig. 1. Molecular structure of **6**.

The structure of $[Fe_2\{\mu\text{-}Ag(PPh_3)\}(\mu\text{-}CO)(CO)_6(\mu\text{-}PBu^t{}_2)]$ (**6**)

Figure 1 shows the molecular structure of **6** with the atomic numbering scheme. Selected bond lengths and angles are given in Table 5.

The core of the molecule consists of a trinuclear cluster built up of two iron atoms and a silver atom which are positioned at the corners of an almost equilateral triangle. The Fe—Fe bond is double-bridged by both a di-tert.-butylphosphido ligand and a carbonyl group. Besides, the Ag atom is coordinated by a triphenylphosphane ligand and to each iron atom three terminal CO groups are attached. Apart from the organic substituents at the P atoms, the molecule has, in rather good approximation, C_s symmetry with a mirror plane containing atoms Ag, C(4), O(4), P(1) and P(2).

The structure of **6** strongly resembles that of the cation in $[Fe_2(\mu\text{-}Ag)(CO)_6\{\mu\text{-}CHC(NHCH_3)(C_6H_5)\}\mu\text{-}PPh_2)]ClO_4 \cdot C_6H_6 \cdot C_6H_5CH_3$[31] with the only relevant difference that the iron atoms are bridged by a carbonyl group instead of a μ-η^1-alkylidene ligand. Bond lengths in the Fe_2Ag triangles (Ag—Fe(1) = 2.685(1), Ag—Fe(2) = 2.703(1), Fe(1)—Fe(2) = 2.682(1) Å for the cation,[31] for **6** cf. Table 5) are substantially the same and differ by less than 0.03 Å. The Fe—P(2) distances within the phosphido bridge of **6** are about 0.05 Å longer compared with those of the cation and accordingly the Fe(1)—P(2)—Fe(2) angle is more acute by 2.6°. The Ag—P bond length in **6** (2.404(2) Å) is in the range normally observed in silver phosphane complexes (e.g. 2.414(4) Å in $[cp(CO)_2Mo\{\mu\text{-}Ag(PPh_3)\}(\mu\text{-}PPh_2)Mn(CO)_4]$[32]).

The three planes defined by the two iron atoms and one of the corresponding atoms bridging them make the following angles: Fe(1), Fe(2), Ag/Fe(1), Fe(2), P(2) 110.8°, Fe(1), Fe(2), Ag/Fe(1), Fe(2), C(4) 134.5°, Fe(1), Fe(2), Ag/Fe(1), Fe(2), C(4) 114.7°. Surprisingly, the interplanar angle between the planes including the ligator atoms with the most

Table 5. Selected bond lengths (Å) and angles (°) in **6** with estimated standard deviations in parentheses

Ag—Fe(1)	2.693(1)	Fe(1)—C(1)	1.817(7)
Ag—Fe(2)	2.670(1)	Fe(1)—C(2)	1.770(9)
Fe(1)—Fe(2)	2.656(1)	Fe(1)—C(3)	1.749(8)
Ag—P(1)	2.404(2)	Fe(1)—C(4)	1.985(7)
Fe(1)—P(2)	2.271(2)	Fe(2)—C(4)	1.942(7)
Fe(2)—P(2)	2.274(2)	Fe(2)—C(5)	1.809(9)
		Fe(2)—C(6)	1.787(8)
		Fe(2)—C(7)	1.767(7)
Fe(1)—Ag—Fe(2)	59.36(2)	Ag—Fe(2)—Fe(1)	60.75(3)
Fe(1)—Ag—P(1)	154.70(5)	Ag—Fe(2)—P(2)	88.05(5)
Fe(2)—Ag—P(1)	145.23(6)	Ag—Fe—C(4)	97.4(2)
Ag—Fe(1)—Fe(2)	59.89(3)	Ag—Fe(2)—C(5)	74.2(2)
Ag—Fe(1)—P(2)	87.55(6)	Ag—Fe(2)—C(6)	74.2(2)
Ag—Fe(1)—C(1)	71.5(3)	Ag—Fe(2)—C(7)	167.7(3)
Ag—Fe(1)—C(2)	79.1(3)	Fe(1)—Fe(2)—P(2)	54.20(5)
Ag—Fe(1)—C(3)	169.6(2)	Fe(1)—Fe(2)—C(4)	48.1(2)
Ag—Fe(1)—C(4)	95.6(2)	Fe(1)—Fe(2)—C(5)	101.7(3)
Fe(2)—Fe(1)—P(2)	54.30(5)	Fe(1)—Fe(2)—C(6)	125.5(2)
Fe(2)—Fe(1)—C(1)	123.3(2)	Fe(1)—Fe(2)—C(7)	131.2(3)
Fe(2)—Fe(1)—C(2)	104.5(2)	P(2)—Fe(2)—C(4)	82.0(2)
Fe(2)—Fe(1)—C(3)	130.4(2)	P(2)—Fe(2)—C(5)	155.5(3)
Fe(2)—Fe(1)—C(4)	46.8(2)	P(2)—Fe(2)—C(6)	97.9(3)
P(2)—Fe(1)—C(1)	98.9(2)	P(2)—Fe(2)—C(7)	101.8(3)
P(2)—Fe(1)—C(2)	158.8(3)	C(4)—Fe(2)—C(5)	83.6(3)
P(2)—Fe(1)—C(3)	97.8(3)	C(4)—Fe(2)—C(6)	171.6(3)
P(2)—Fe(1)—C(4)	81.2(2)	C(4)—Fe(2)—C(7)	91.3(3)
C(1)—Fe(1)—C(2)	92.5(3)	C(5)—Fe(2)—C(6)	93.4(4)
C(1)—Fe(1)—C(3)	98.8(4)	C(5)—Fe(2)—C(7)	98.3(4)
C(1)—Fe(1)—C(4)	167.1(3)	C(6)—Fe(2)—C(7)	96.9(4)
C(2)—Fe(1)—C(3)	98.0(4)	Fe(1)—P(2)—Fe(2)	71.51(6)
C(2)—Fe(1)—C(4)	83.8(3)		
C(3)—Fe(1)—C(4)	94.0(3)		

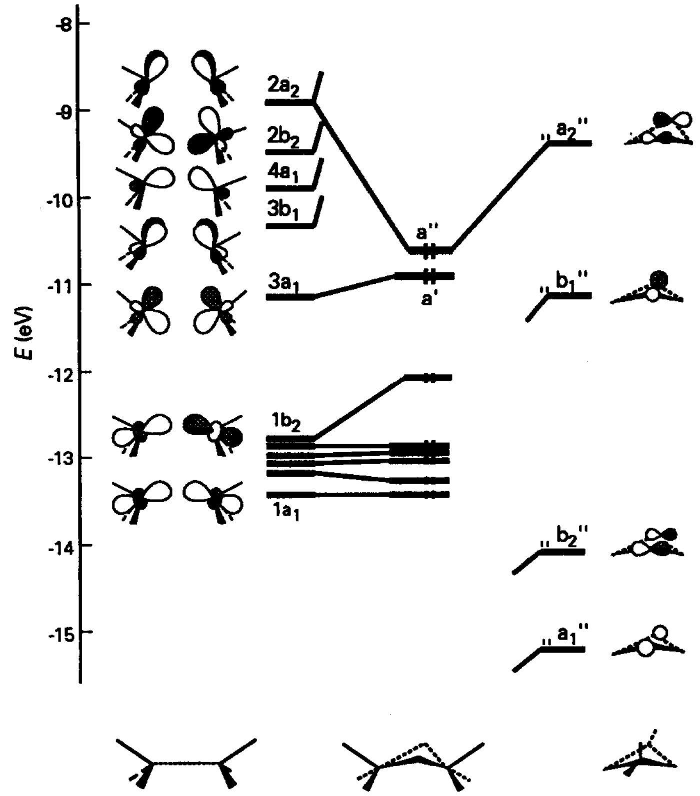

Fig. 2. Molecular orbital diagram of the anion $[Fe_2(\mu\text{-}CO)(CO)_6(\mu\text{-}PH_2)]^-$ build up from a $Fe_2(CO)_6$ fragment and the two bridging ligands CO and PH_2^-. The orbitals of both fragments have been donated according to the point group C_{2v} to make clear the orbital interactions. The orbitals of the anion itself have been donated according to C_s.

bulky substituents (Ag, P(2)) is the smallest. A comparison between the terminal CO groups and the μ-CO with regard to their bond lengths gives the expected result: the former have longer C—O distances (mean value 1.146(8) Å compared with C(4)—O(4) = 1.191(8) Å) but shorter Fe—C distances.

The six Fe—C—O angles expected to be nearby 180° can be classified into two groups: four with values of about 176° and two (at C(1) and C(7)) with stronger deviations from linearity (about 170°). The latter belong to CO groups in *trans*-position to C(4) and the bend might arise from the influence of the triphenyl-phosphane substituent at the silver atom.

The crystal packing consists of isolated molecules without special intermolecular contacts. Preliminary X-ray investigations of the analogous clusters **5** and **7** gave no indication of isomorphism with **6**.

Molecular orbital calculations

The ambident nucleophilic reactivity of the anions $[Fe_2(\mu\text{-}CO)(CO)_6(\mu\text{-}PR_2)]^-$ as described in the resonance formulae A and B should be reflected in the electronic structure of the compound. Therefore, we carried out Extended Hückel molecular orbital calculations[33,34] to examine the sources for this ambivalence.*

Figure 2 shows the molecular orbital diagram of the anion built up from the well-known $Fe_2(CO)_6$ fragment[35] and the two bridging ligands CO and PH_2^-, the latter being a model for the phosphido ligands PR_2^-. The di-iron fragment orbitals $2a_2$, $2b_2$, $4a_1$ and $3b_1$ interact with the symmetric and antisymmetric combinations of the σ and π orbitals of the coordinating atoms to form four metal-bridge bonds. Caused by the different energetic position of the phosphido orbitals and the CO orbitals the symmetric combinations of the ligand orbitals are mainly localized at the phosphorus, whereas the antisymmetric combinations are mainly CO in character. The two highest occupied anion orbitals a'' and a' are schematically shown in Fig. 3. The

---

* Standard parameters were used for the calculations. The geometries for the models match that of the X-ray diffraction studies reported in ref. 1 and in the present paper.

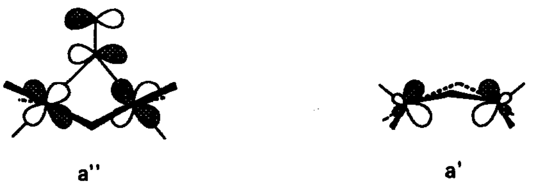

Fig. 3. The two highest occupied anion orbitals.

HOMO *a''* is the bonding combination between the orbitals $2a_2$ of the di-iron fragment and the π^* orbital of the carbonyl ligand. It represents one of the four metal-bridge bonds. The orbital *a'* is not influenced by interactions with the bridging ligands. It is considered to indicate the bent Fe—Fe bond in the anion, resembling that described for the $[Fe_2(CO)_6(\mu\text{-}PR_2)_2]$ system.[36,37] Both orbitals *a'* and *a''*, can act as donor orbitals towards nucleophiles. Figure 4 represents the metal-based reactivity against a "third bridging ligand" $[M(PR_3)]^+$ with a d^{10}-configurated metal ion M^+ (M = Cu, Ag, Au). The LUMO of $[M(PR_3)]^+$ is a σ-acceptor orbital that interacts with the anion orbital *a'* to form one additional metal-bridge bond. This description of the bonding within the Fe_2M core of complexes **5**–**7** is in accordance with the bonding situation in heteronuclear gold-metal clusters containing a μ-bridging $Au(PR_3)$ fragment which is generally said to involve a three-centre two-electron bond between the two metal atoms and the gold atom.[38] Thus, the 46 electron count of these triangular clusters follows from the electron deficiency of this bond.

Although the structure of the hydride complex $[Fe_2(\mu\text{-}CO)(CO)_6(H)(\mu\text{-}PBu^t{}_2)]$ (**4a**) could not be ascertained, this complex might have a similar molecular and electronic structure as discussed for complexes **5**–**7** due to the isolobal analogy of H^+ and $[M(PPh_3)]^+$ (M = Cu, Ag, Au).

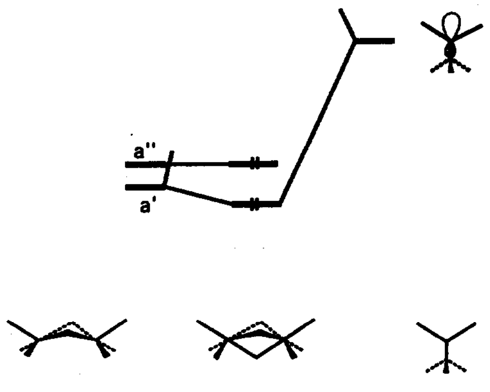

Fig. 4. Schematic plot of the bonding interaction between the anion orbital *a'* and the LUMO of a bridging $[M(PR_3)]^+$ group (M = Cu, Ag, Au).

The oxygen-based nucleophilicity of anions **3** is understandable by inspecting orbital *a''* (Fig. 3). This orbital can be considered to be mainly an oxygen lone pair orbital that is able to donate electronic density from oxygen into the acceptor orbital of e.g. a $CR_3{}^+$ group. This is confirmed by the net charges (Mulliken population analysis) of the atoms in the anion model compound: $q(Fe) = 0.22$, $q(PH_2) = 0.02$, $q(C_{term}) = 0.67$ (mean value), $q(O_{term}) = -0.78$ (mean value), $q(C_{bridge}) = 0.20$, $q(O_{bridge}) = -1.03$, i.e. the carbonyl bond in the bridging CO is highly polar corresponding to formula **B**.

Acknowledgements—B.W. thanks Dr E. P. Kyba, Fort Worth, Texas, for providing a copy of parts of T. Osterloh's thesis, and Dr R. T. Baker, Wilmington, Delaware, for comments concerning the synthesis of complexes **3**.

REFERENCES

1. W. T. Osterloh, Ph.D. thesis. University of Texas, Austin, TX (1982); University Microfilms International Ann Arbor, MI (1982).
2. R. T. Baker, J. C. Calabrese, P. J. Krusic, M. J. Therien and W. C. Trogler, *J. Am. Chem. Soc.* 1988, **110**, 8392.
3. R. T. Baker, P. J. Krusic, J. C. Calabrese and D. C. Roe, *Organometallics* 1986, **5**, 1506.
4. P. J. Krusic, R. T. Baker, J. C. Calabrese, J. R. Morton, K. F. Preston and Y. LePage, *J. Am. Chem. Soc.* 1989, **111**, 1262.
5. M. Field, O. Stelzer and R. Schmutzler, *Inorg. Synth.* 1973, **14**, 4.
6. K. Issleib and W. Seidel, *Chem. Ber.* 1959, **92**, 2681.
7. M. P. Brown and H. B. Silver, *Chem. Ind.* 1961, 24.
8. G. W. Parshall, *Inorg. Synth.* 1974, **15**, 191.
9. J. P. Collmann, R. G. Finke, P. L. Matlock, R. Wahren, R. G. Komoto and J. J. Baumann, *J. Am. Chem. Soc.* 1978, **100**, 1119.
10. R. G. Finke and T. N. Sorrell, *Org. Synth.* 1980, **59**, 102.
11. J. K. Ruff and W. J. Schlientz, *Inorg. Synth.* 1974, **15**, 84.
12. G. Costa, E. Reisenhofer and L. Stefani, *J. Inorg. Nucl. Chem.* 1965, **27**, 2581.
13. A. Pernick and M. Ardon, *J. Am. Chem. Soc.* 1975, **97**, 1256.
14. A. Davison and J. E. Ellis, *J. Organomet. Chem.* 1972, **36**, 113.
15. W. Ehrl and H. J. Vahrenkamp, *J. Organomet. Chem.* 1963, **63**, 389.
16. C. J. Gilmore, *J. Appl. Cryst.* 1984, **17**, 42.
17. P. T. Beurskens, W. P. Bosman, H. M. Doesburg, R. O. Gould, Th. E. M. van den Hark, P. A. J. Prick, J. H. Nordiik, G. Beurskens and V. Parthasarathi, DIRDIF, Direct methods for difference structures (Technical report 1984/1), Crystallography Laboratory, Toernooiveld, Netherlands (1984).

18. *International Tables for X-ray Crystallography*, Vol. IV, p. 71. The Kynoch Press, Birmingham, England (1974).
19. TEXSAN-TEXRAY *Structure Analysis Package*, Molecular Structure Corporation (1985).
20. P. M. Treichel, W. K. Dean and W. M. Douglas, *Inorg. Chem.* 1972, **11**, 1609.
21. P. M. Treichel, W. K. Dean and J. C. Calabrese, *Inorg. Chem.* 1973, **12**, 2908.
22. M. Ferrer, R. Reina, O. Rossell, M. Seco and X. Solans, *J. Chem. Soc., Dalton Trans.* 1991, 347.
23. D. Seyferth, G. B. Womack, C. M. Archer and J. C. Dewan, *Organometallics* 1980, **8**, 430.
24. P. E. Garrou, *Chem. Rev.* 1981, **81**, 229.
25. A. J. Carty, *Adv. Chem. Res.* 1982, **196**, 163.
26. G. L. Geoffroy, *Organometallics* 1983, **2**, 53.
27. I. D. Salter, *Adv. Organomet. Chem.* 1989, **29**, 249.
28. B. Delavaux, B. Chandret, F. Dahan and R. Poilblanc, *J. Organomet. Chem.* 1986, **317**, 69.
29. T. C. Gibb, R. Greatrex and N. N. Greenwood, *J. Chem. Soc. A* 1968, 890.
30. T. C. Gibb, R. Greatrex, N. N. Greenwood and D. T. Thompson, *J. Chem. Soc. A* 1967, 1663.
31. G. N. Mott, N. J. Taylor and A. J. Carty, *Organometallics* 1983, **2**, 447.
32. A. D. Horton, M. J. Mays, T. Adatia and M. McPartlin, *J. Chem. Soc., Dalton Trans.* 1988, 1683.
33. R. Hoffmann and W. N. Lipscomb, *J. Chem. Phys.* 1962, **36**, 2179.
34. R. Hoffmann, *J. Chem. Phys.* 1963, **39**, 1397.
35. R. H. Summerville and R. Hoffmann, *J. Am. Chem. Soc.* 1979, **101**, 3821.
36. B. K. Teo, M. B. Hall, R. F. Fenske and L. F. Dahl, *Inorg. Chem.* 1975, **14**, 3103.
37. E. L. Anderson, T. P. Fehlner, A. E. Foti and D. R. Salahub, *J. Am. Chem. Soc.* 1980, **102**, 7422.
38. K. P. Hall and D. M. P. Mingos, *Prog. Inorg. Chem.* 1984, **32**, 277.